

Design of Plano-Convex Lens Antenna Fed by Microstrip Patch Considering Integration with Microwave Planar Circuits

Seung-Gab Yu · Dong-Min Yeon · Yong-Hoon Kim

Abstract

In this paper, the plano-convex lens antenna fed by a single patch is studied for a microwave remote-traffic monitoring sensor with constraints of small size and low cost. Measurement of an AUT (Antenna Under Test) involves the considerations of a triangular groove for matched layer and metallic shielding effects. A formulation for extracting the parameters of a plano-convex lens antenna, based on geometrical optics, is introduced using Fermat's principle of the equi-phased ray condition. Teflon ($\epsilon_r=2.0$) is chosen as a material of a plano-convex lens antenna for adjustment of aberrations on the lens surfaces automatically. A fabricated plano-convex lens shows 3-dB beamwidth of 7.5 degree and side-lobe level of -29 dB with an aperture distribution of the parabolic-squared taper on pedestal. This lens supports easier integration with the planar microwave circuits by using a microstrip single patch as a primary feeder of the lens antenna.

I. INTRODUCTION

In the radar or mobile communication fields, there have been many different approaches for the antenna to have narrow beamwidth, low side-lobe level and high beam efficiency characteristics. Although various reflector antenna, microstrip array and horn antenna have been suggested to obtain the desired antenna performances, several drawbacks of each antennas cause problems to apply in practical application. For example, reflector type involves a problem of a feed blockage, and microstrip array antenna has an undesired feed line radiation. As needs for a high-speed data transmission have been increased, the lens antenna is recommended as one of good candidates since it supports low side-lobe characteristics with small aperture size. Also, there is no feed blockage and insure tolerance of surface irregularity compared to conventional antennas. This type of lens antenna was used to avoid the feed blockage in a reflector by using a ray-through structure and to compensate the phase distortion in a large aperture of the horn antenna caused by reducing the extended length of a side-wall of horn. But a size of the lens is so big that could not be used practically in the low frequency band. The drawbacks of a lens antenna can be eliminated in the millimeter-wave bands due to the shorter electrical wavelength. In this paper, plano-convex lens antenna fed by single patch antenna is suggested for easier combination with other planar microwave circuits in the microwave remote-traffic monitoring sensor (MRTMS) that we developed. Required bandwidth of the system is 250 MHz at the

center frequency of 24 GHz.

II. RADIATION PATTERN OF PLANO-CONVEX LENS ANTENNA

The entire procedures to extract the lens parameters of diameter, focal length and thickness are described in Fig. 1. In the Fig. 2, $A(\theta)$ denotes radiated power per unit solid angle from the point source in the θ -direction. $P(\rho)$ is the corresponding power per unit area in the aperture with a function of a distance from axis, $\rho (= R \sin \theta)$. From the relationship between $A(\theta)$ and $P(\rho)$ in the aspect of a power conservation law, general formulation of an aperture distribution can be deduced as follows assuming no reflective loss in the intermediate medium^[3].

$$P = 2\pi\rho d\rho P(\rho) = 2\pi \sin\theta d\theta A(\theta) \tag{1}$$

Using a relationship of $\rho = R \sin \theta$ and equation (1), aperture amplitude distribution will be represented as,

$$P(\rho) = -\frac{\sin\theta}{\rho} \left(\frac{d\theta}{d\rho} \right) A(\theta) = \frac{1}{R} \left(\frac{1}{d\rho/d\theta} \right) A(\theta) \tag{2}$$

$$\frac{P(\rho)}{A(\theta)} = \frac{(n \cos \theta - 1)^3}{(n-1)^2 L^2 (n - \cos \theta)} \tag{3}$$

A parameter, n , means refractive index of a lens material satisfying $n = \sqrt{\epsilon_r}$, and L is the focal distance from an aperture of the primary feeder to the apex of a lens antenna. The equation (4) represents the normalization of a maximum power

Manuscript received March 31, 2001; revised May 16, 2001.

The authors are with the Dept. of Mechatronics, Kwangju Institute of Science and Technology(K-JIST)

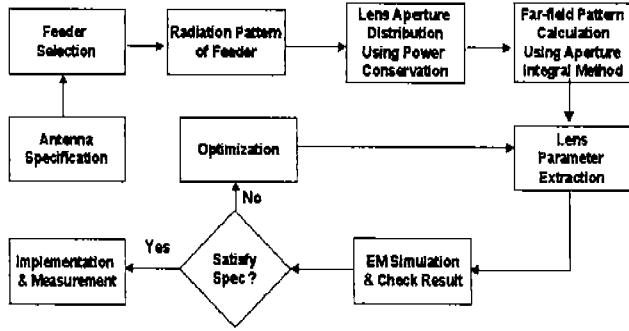


Fig. 1. Design procedures of plano-convex lens antenna.

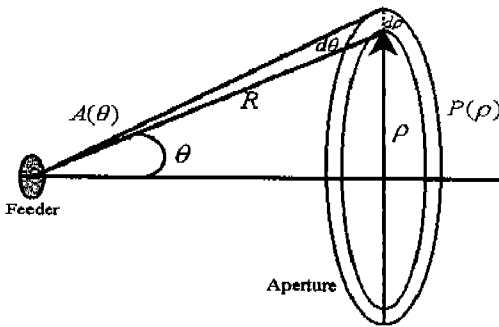


Fig. 2. Power conservation property between a primary feeder and a lens antenna.

with $1/L^2$ at $\theta = 0^\circ$ for analyzing the radiation pattern from a constructed aperture distribution.

$$\left(\frac{P(\rho)}{A(\theta)}\right) = \frac{(n \cos \theta - 1)^3}{(n-1)^2(n - \cos \theta)} \quad (4)$$

In the aperture plane of the lens, the field intensity ratio is equal to the square root of equation (4), thus we can obtain equation (5).

$$E(\rho) = \sqrt{\frac{(n \cos \theta - 1)^3}{(n-1)^2(n - \cos \theta)}} F(\theta) \quad (5)$$

$$F(\theta) = \frac{\sin\left(\frac{k_0 W}{2} \cos \theta\right)}{\frac{k_0 W}{2} \cos \theta} \sin \theta \quad (6)$$

where,

$$k_0 = w\sqrt{\mu\epsilon} = \frac{2\pi f_r}{c} \quad (7)$$

$E(\rho)$ represents amplitude distribution of a lens aperture and $F(\theta)$ is the radiated field intensity in the direction of θ ^{[3],[4]}. The phase distribution on the lens aperture is constructed uniformly due to the surface shaping of a plano-convex lens using an equi-phased ray condition on the secondary aperture.

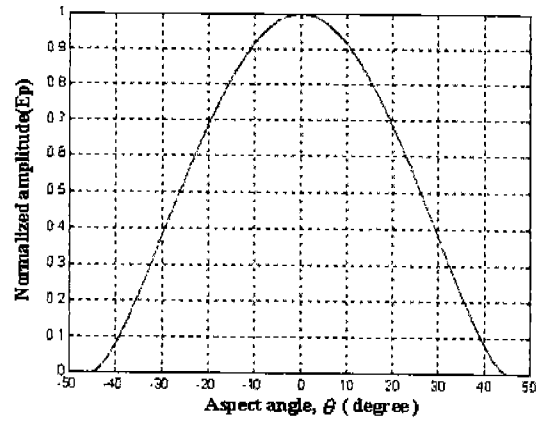


Fig. 3. Amplitude distribution on lens aperture ($n = \sqrt{2}$).

The amplitude distribution on a secondary aperture of lens is shown in Fig. 3 with respect to an aspect angle of θ , which is depicted based on the equation (5)~(7). The desired edge illumination can be formed by a proper focal length with a smaller aspect angle of θ rather than the asymptotic angle of θ_0 as shown in Fig. 3 and Fig. 4.

III. SYNTHETIC EXTRACTION OF LENS PARAMETERS

Following formulas describe how we can adopt Fermat's principle to the lens surface modeling. Using a phase equality between a central ray and a arbitrary directional ray in Fig. 4, the path length of the each rays can be represented as following equations from (8) to (12) assuming $n > 1$ ^[5],

$$(OP) = (OQ) + n(QQ') \quad (8)$$

$$\frac{R}{\lambda_0} = \frac{L}{\lambda_0} + \frac{R \cos \theta - L}{\lambda_d} \quad (9)$$

Multiplying by λ_0 ,

$$R = L + n(R \cos \theta - L) \quad (10)$$

$$R = \frac{(n-1)L}{n \cos \theta - 1} \quad (11)$$

$$\theta_0 = \cos^{-1}\left(\frac{1}{n}\right) \quad (12)$$

R and θ_0 represent radial distance and asymptotic line of hyperbolic shape in polar coordinates, respectively. The equation (13) is a result of coordinate transformation from the polar coordinates to the rectangular coordinates system, and it represents hyperbolic function^[5].

$$\left[z - \frac{n}{n+1}L\right]^2 - \frac{\rho^2}{n^2-1} = \frac{L^2}{(n+1)^2} \quad (13)$$

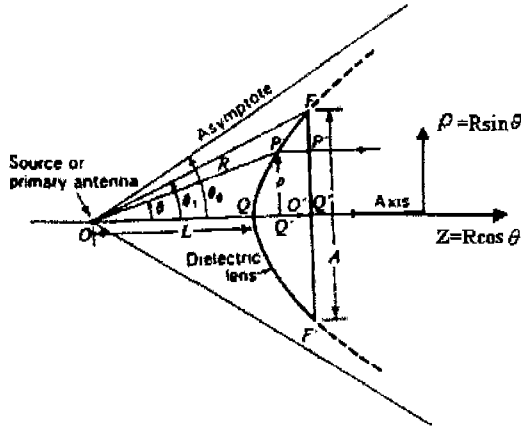


Fig. 4. Ray trajectory diagram of plano-convex.

Table 1. Extracted lens parameters

L / D	T / D	Depth / Pitch
0.46	0.34	0.65

$$HPBW = k \frac{\lambda_g}{0.5D} \quad (14)$$

Lens parameters of diameter (D), focal length (L) and thickness (T) are extracted under the aperture distribution of a parabolic-squared taper on pedestal, and values are summarized in Table 1^[6]. Diameter of the lens was computed approximately from the information of θ in the equation (5) and HPBW in the equation (14) according to an edge illumination value of -8 dB from the peak level that constrains a value of k ^[6]. After calculating D , $L + T$ is computed using a simple geometrical relationship of the equation (15) instead of computing the L and T independently. Equation (15) is simply deduced from the geometrical relationship among the lens parameters as shown in Fig. 4.

$$\theta_1 = \tan^{-1} \left(\frac{0.5D}{L+T} \right) \quad (15)$$

The parameter of θ_1 is the known value since it is the angle passing through edge of the lens aperture as shown in Fig. 4. D is the also known value from previous calculation. An information of the central thickness, T , is separated from $L + T$, using the equation (16)^[7].

$$T = \frac{1}{n+1} \left(\sqrt{L^2 + \frac{(n+1)D^2}{4(n-1)}} - L \right) \quad (16)$$

IV. TRIANGULAR GROOVE FOR MATCHED LAYER

The material discontinuity between a lens and an air causes the reflection loss and a degradation of a side-lobe performance

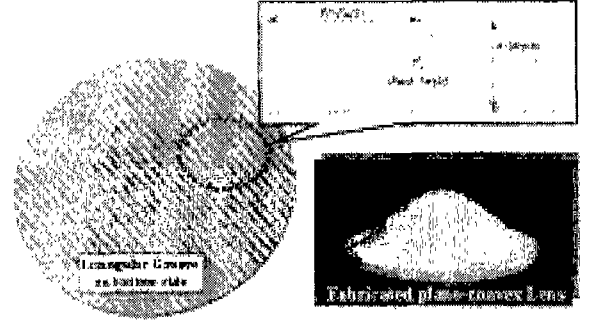


Fig. 5. Triangular groove configuration on flat aperture.

due to the mismatching. Even though a quarter-wave length thin film layer has been suggested to correct the mismatching problem in early times, there have existed some problems in the manufacturing that is hard to obtain a uniformity of thickness on the deposited layer and difficult to utilize the adequate materials. Another technique of the groove has been suggested using an electrical property of the effective quarter-wave transformation by digging the rectangular or triangular hole on the lens surface as shown in Fig. 5. In this paper, triangular groove is chosen for a groove on the flat aperture side because of the less sensitivity for a manufacturing error compared to the rectangular one. Since Raguin and Morris already presented the calculation of the groove parameters, we present only the final results of their study, here^[9].

$$P < \frac{\lambda_{a0}}{\sqrt{\epsilon_{re}} + \sqrt{\epsilon_{r0}} |\sin \theta_i|} \quad (17)$$

ϵ_{re} and ϵ_{r0} mean permittivity of an utilized material for lens and air, respectively. θ_i is the incident angle into the grooved aperture. θ_i should be zero in equation (17) since there is only normal incident wave on the flat side of plano-convex lens. The depth is computed in order to have the quarter-wave length in the utilized material of the lens. The pitch is designed to have $\lambda_0/20$ ^[10]. The Ratio of a pitch (P) length and depth (d) is presented in Table 1.

V. SIMULATION AND EXPERIMENT RESULTS

When choosing a material for the plano-convex lens, there are several considerations of permittivity, reflective loss and manufacturing capability. In this works, Teflon ($\epsilon_r=2$) is chosen for a small loss and a capability to avoid aberration on aperture automatically^[11]. A linearly polarized rectangular patch antenna were fabricated at the center frequency of 24 GHz using RO4003 substrate. Simulated radiation pattern of the patch antenna is shown in the Fig. 6. Measured radiation pattern of an implemented single patch couldn't be obtained due to the

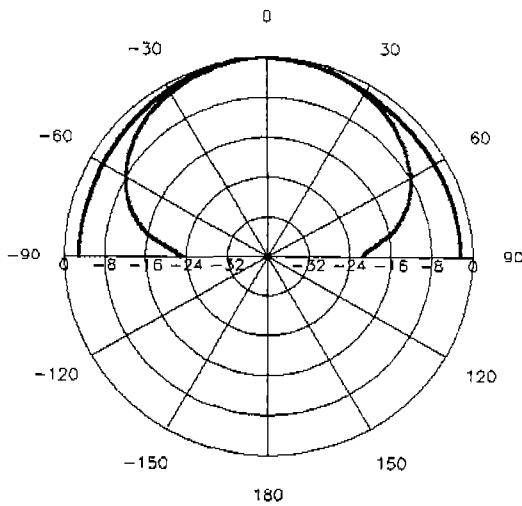


Fig. 6. Simulated radiation pattern of linearly polarized rectangular single patch antenna at 24 GHz.

measurement system. Measured return loss within 250 MHz bandwidth at the center of 24 GHz is under the -10dB. EM Simulation of axially symmetrical plano-convex lens antenna fed by single patch is performed using the HFSS5.4 with extracted dimension of D , L and T at 24 GHz. Simulated and measured data are shown in Fig. 7 and Fig. 8(a) when L/D is 0.46. Due to the fabrication tolerance of a lens antenna, measured data at $L/D=0.46$ does not give the best performance. Since the profile of a hyperbolic surface of the plano-convex lens could not be identified exactly in the fabrication, some additional measurements would be required to find the best operation point. The best performance was obtained when locating the focal length at $L/D=0.44$ with fixed $T/D=0.34$ as shown in Fig. 8(b). Table 2 represents the summary of a simulation and a measurement.

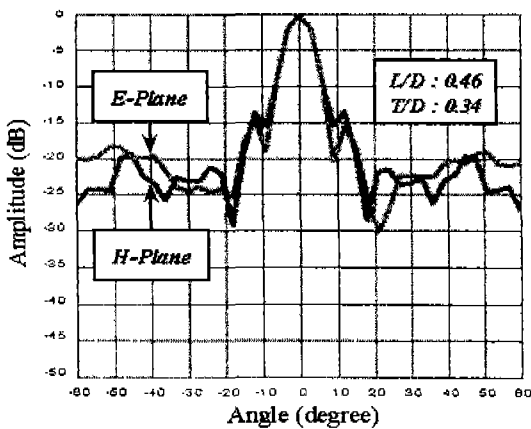
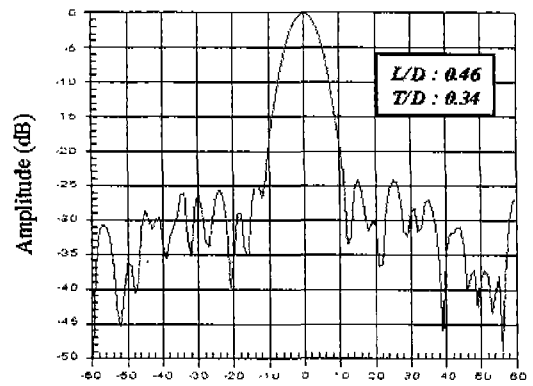
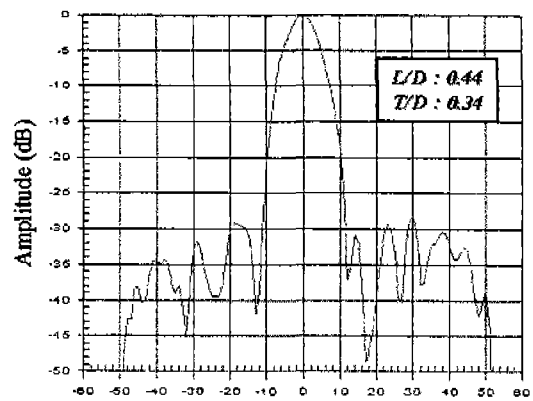


Fig. 7. Simulated radiation pattern of single patch fed plano-convex lens antenna at 24 GHz ($L/D=0.46$).



(a) $L/D = 0.46$, $T/D = 0.34$



(b) $L/D = 0.44$, $T/D = 0.34$

Fig. 8. Measured radiation pattern of single patch fed plano-convex lens antenna at 24 GHz.

Table 2. Summary of simulated and measured data

	Simulation ($L/D=0.46$)	Measurement ($L/D=0.46$)	Measurement ($L/D=0.44$)
HPBW	8 degree	8 degree	7.5 degree
Side lobe level	-13 dB	-24 dB	-29 dB

Why the side-lobe level of simulation differs from the measured one could be explained with a mesh problem when representing a perfect hyperbolic surface of the plano-convex lens in the HFSS environment. Approximated representation of a hyperbolic surface of the lens with rotational segment results in different side-lobe characteristics compared to the measured one.

We see relatively small degradation of the side-lobe level in a triangular grooved lens due to the manufacturing error, and radiation pattern is presented in Fig. 9. Metallic shielding effects are also observed experimentally, and measured data is present-

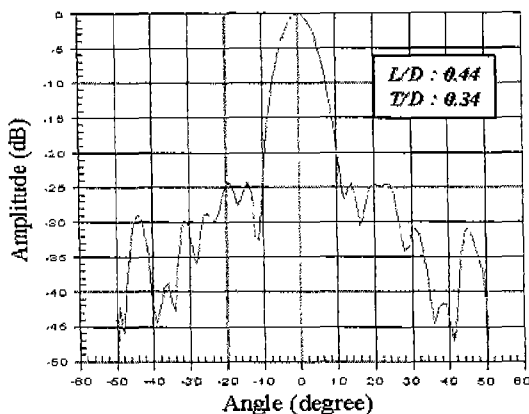


Fig. 9. Measured radiation pattern of single patch fed triangular grooved lens antenna at 24 GHz ($L/D=0.44$).

ted in Fig. 10. In the shielded environment, a rectangular shielding form is more suitable in the aspect of side-lobe reduction compared to cylindrical one. Although we did not perform the numerical analysis to analyze a triangular groove and metallic shielding effect yet, we are trying to solve above problems presently using a numerical method of the ray tracing algorithm.

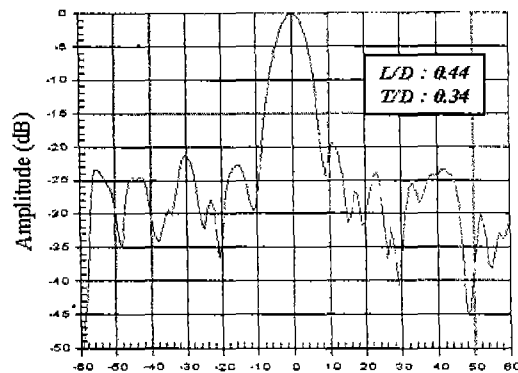
VI. CONCLUSION

In this paper, a plano-convex lens antenna fed by a single patch is suggested for the easier integration with microwave planar circuits in MRTMS. The best performance of a designed plano-convex lens antenna is measured at $L/D=0.44$, $T/D=0.34$ with a 3-dB beamwidth of 7.5 degree and peak side-lobe level of -29 dB. Although these results of a fabricated lens are measured at the shorter focal position rather than a calculated value, it is in good agreement with the computation considering the fabrication tolerance. The effects of a triangular groove and a metallic shield are measured for matching layer and packaging, respectively. Rectangular metallic shield shows better performance rather than cylindrical one. In the next publication, we will verify the measured performance of a triangular groove and metallic shielding effects with numerical analysis of ray tracing method.

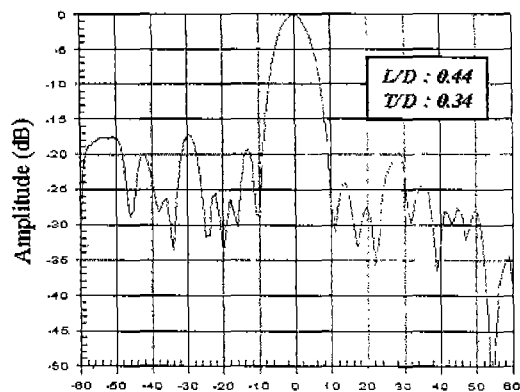
This work was supported by Brain Korea 21 project.

REFERENCES

[1] Gabriel M. Rebeiz, "Millimeter-wave and terahertz integrated circuit antennas", *Proceedings of IEEE*, vol. 180, no. 11,



(a) Rectangular shield



(b) Cylindrical shield

Fig. 10. Shielding effects on radiation pattern of plano-convex lens at 24 GHz.

- pp. 1748-1770, November, 1992.
- [2] C. J. Sletten, *Reflector and Lens Antennas*, chap. 5, A/H, 1988.
- [3] S. Silver, *Microwave Antenna Theory and Design*, M.I.T. Radiation Laboratory Series, vol. 12, chap. 11, MC-Graw-Hills, 1949.
- [4] I. J. Bahl, *Microstrip Antennas*, chap. 2, 2nd Ed., A/H, 1982.
- [5] Kohei Hongo, "Radiation characteristics of Plano-Convex lens antennas", *Radio Science*, vol. 31, no. 5, pp. 1025-1035, 1996.
- [6] Warren L. Stutzman and Gary A. Thiele, *Antenna Theory and Design*, Chap 8, John Wiley & Sons, 1981.
- [7] Y. T. Lo, *Antenna Handbook Vol II Antenna Theory*, chap. 16, pp. 16-10, Van Nostrand Reinhold, 1993.
- [8] A. R. Kerr "Program 'Scatter' for analysis of dielectric matching layers", *Electronics Division Technical notes*, 1989.
- [9] Daniel H. Raguin and G. Michael Morris, "Analysis of

anti-reflection structure surfaces with continuous one-dimensional surface profiles", *Applied Optics*, vol. 32, no. 14, 10, May, 1993.

[10] Guillermo F. Delgado, "Scanning properties of teflon

lenses", *M/W and Optical Tech. Letters*, pp. 271-273, 1996.
[11] J. A. Park, "The design of quasi-optics for dualchannel SIS receiver", *J. Astron. Space Sci.*, vol. 14, pp. 67-79, 1997.

Seung-Gab Yu



was born in Seoul, Korea, on August 1976. He received the B. S degree in Avionics from Hankuk Aviation Univ. in 1999. In 1999, he joined Kwang-Ju Institute of Science and Technology (K-JIST) as a candidate for the M.S. degree. He is currently working on developing low noise amplifier and optimum structure of dielectric aperture antenna suitable

for MMOF (Millimeter-wave over fiber) system combining MMIC technology with optical fiber for high-speed data communication.

Yong-Hoon Kim



received the B.S. degree from Kyung-Hee Univ. in 1974, the M. S. degree from Yonsei Univ. in 1976, Korea, and Dr.-Ing. degree from Stuttgart Univ. in 1990, Germany. In 1990, he joined the Korea Aerospace Research Institute and worked as a department head of Space Application Technology, Avionics and Space Payload. From August 1994 to February 1995 he worked as a

research fellow in ARINC Research Co. He joined Kwang-Ju Institute of Science and Technology (K-JIST) as a professor in February 1995. Since then, he has been interested in the development of microwave, millimeter-wave components and systems, millimeter-wave communication and imaging radar system, remote sensing system for airborne and spaceborne. He is currently working on the high-speed indoor communication system and interferometric synthetic aperture imaging radiometer. He is a member of MTT, IEEE and KSRC, KITE in Korea.

Dong-Min Yeon



received the B. S degree in Electronics from KOREA Univ., SEOUL in 1999. In 1999, he joined the Kwang-Ju Institute of Science and Technology (K-JIST) as a candidate for the M. S. degree. Current research topic is mm-wave band frequency synthesizer including VCO and N-fractional frequency divider for PLL. He is now working on developing Injection Locking

Oscillator for mm-wave band frequency division in PLL.